Polymer Journal, Vol. 37, No. 6, pp. 404–412 (2005)

Helix–Coil Transition and Micellar Structure of Poly(ethylene glycol)-*block*-Poly[N^5-(2-hydroxyethyl) L-glutamine] in Cyclohexanol/Water Mixed Solvents

Katsuhiro INOMATA,† Minako ITOH, and Eiji NAKANISHI

Department of Materials Science and Engineering, Nagoya Institute of Technology, Gokiso-cho, Showa-ku, Nagoya 466-8555, Japan

(Received November 29, 2004; Accepted March 11, 2005; Published June 15, 2005)

ABSTRACT: Structure analysis of associated micelles formed by polypeptide-based diblock copolymer PEG-*b*-PHEG, consisting of poly(ethylene glycol) (PEG) and poly[N^5-(2-hydroxyethyl) L-glutamine] (PHEG), in dilute solution has been investigated. Cyclohexanol/water mixed solvent was used as selective solvent for PEG-*b*-PHEG, in which PHEG forms associated domains. Circular dichrorism measurements revealed that PHEG block changes its conformation from α-helix state to random coil state with increase of water content in the mixed solvent from 2.3 to 12.1 wt %. Apparent molecular weight and radius of gyration of associated micelles were derived by light scattering measurements, and most plausible structure of the micelle was evaluated. When the water content is small and helix content of PHEG is almost 100%, a cylindrical micelle with large association number was suggested, and a vesicle-like hollow cylindrical micelle with large diameter was proposed. With the increase of water content and decrease of helix content, association number of the micelle decreased and a core-corona type cylindrical micelle with densely packed PHEG core was plausible. These structure changes of the micelles were interpreted by possible chain packing of α-helical and randomly-coiled PHEG and curvature of PHEG core domain. The obtained results indicate that the conformation and packing manner of the core-forming chain strongly influence the structure of the diblock copolymer micelles. [DOI 10.1295/polymj.37.404]

KEY WORDS Micelle / Helix–Coil Transition / Polypeptide-based Diblock Copolymer / Rod–Coil / Molecular Packing /

A-block-B diblock copolymers are known to self-assemble to associated micelles in selective solvent.[1,2] In a case that solvent is poor for A block and good for B block, A block forms associated core, and B block is dissolved in solvent and acts as corona of micelle. With depending on solvent quality, temperature, concentration, and molecular structure such as molecular weight, block composition and rigidity, the micellar structure is reported to exhibit various morphologies.[3–10] Structure change of polystyrene-*block*-poly(dimethylsiloxane) micelles with increasing solution temperature was reported in detail by Iyama and Nose.[3,4] Zhang and Eisenberg[5–7] investigated multiple morphological changes in aggregates of amphiphilic block copolymers such as spheres, rods, lamellae, vesicles and so on.

Rod–coil block copolymers, which consist of a rigid rod block and a flexible coil block, have recently attracted considerable attention because of its ability to self-assemble and liquid crystalline nature of the rod block.[11–13] Flory's lattice theory for rigid-rod molecules[14,15] shows that nematic ordering of the rod molecule is preferred in order to increase packing entropy in concentrated solution. Theoretical studies for association of rod–coil diblock copolymers also predicted that rod blocks are packed with its long axis aligned in associated domain.[16–18] Interface between rod- and coil-segregated domains is sharp because of their imcompatibility, thus the coils have to stretch more and more, which results in increase of free energy for the associate. The balance of these free energy terms determines the structure of the associate as well as the packing manner of rods. Similar considerations are also applicable to rod–coil block copolymer dissolved in selective solvent, which is good for coil and poor for rod, because poor solvent is strongly rejected from rod-associated core and coils are well-swollen in good solvent. Monte Carlo simulation by Adriani *et al.*[19] suggested that stiffness of insoluble block in diblock copolymer decreases its critical micelle concentration (cmc) and increases micellar size. The decrease in cmc was interpreted as arising from conformational contribution to effective χ parameter, which is due to an increased number of contact between insoluble block and solvent molecules. There have been reported some experimental observations for self-assembled associates of rod–coil diblock copolymers in selective solvent.[20–29] However, there have been only limited studies on effects of chain rigidity of constituent blocks on micellar properties

†To whom correspondence should be addressed (E-mail: inomata.katsuhiro@nitech.ac.jp).

such as stability and structure.

For a purpose to investigate the effect of chain rigidity, polypeptide is suitable as rod block because some polypeptides are known to exhibit conformational transition between rodlike helical structure and random-coil state with depending on surrounding condition. Harada *et al.* reported an effect of helix–coil transition of polypeptide-containing diblock copolymer on its association behavior.[20] Micelle-like dimer formation of poly(ethylene glycol)-*block*-poly(L-lysine) (PEG–P(Lys)) in aqueous medium was suggested to be synchronized with the coil-to-helix transition of poly(Lys) induced by pH change of solvent. However, this block copolymer was molecularly dissolved when poly(Lys) was in random-coil state, therefore, micellar structure change induced by helix–coil transition was not observed.

Poly[N^5-(2-hydroxyethyl) L-glutamine] (PHEG) is nonionic water-soluble polypeptide, and known to occur helix–coil transition in aqueous alcohol such as methanol/water mixed solvent.[30–33] It has been reported that PHEG conformation is in random-coil state in pure water and changes to α-helix with increasing alcohol content of the mixed solvent. If PHEG-containing diblock copolymers are dissolved in aqueous alcohol that is poor for PHEG block, chain rigidity of the core-forming insoluble block is possibly changed by its helix–coil transition induced by changing solvent composition. In this study, we have prepared polypeptide-based diblock copolymer, poly(ethylene glycol)-*block*-poly[N^5-(2-hydroxyethyl) L-glutamine] (PEG-*b*-PHEG, see Figure 1). As a selective solvent, cyclohexanol/water mixed solvent was used: poly(ethylene glycol) (PEG) is soluble in both solvent, and PHEG cannot be dissolved in cyclohexanol but is soluble in water. Therefore, control of rigidity of core-forming PHEG block is expected to be possible by changing the solvent composition of cyclohexanol/water. As described above, conformational change of diblock copolymer from coil–coil to rod–coil will considerably affect its micellar structure when the rod is core-forming block because chain packing manner in the core changes drastically. Helix–coil transition of PHEG block in self-assembled micelles formed by PEG-*b*-PHEG, and structure change of the micelles induced by the conformational transition of core-forming block will be described.

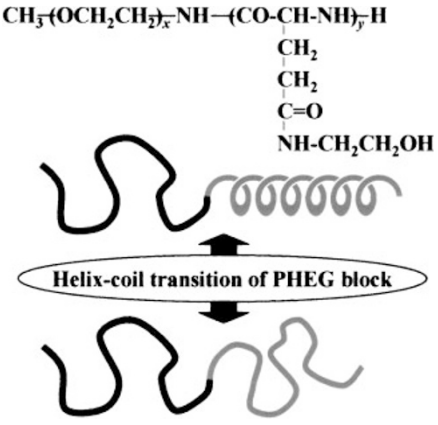

Figure 1. Chemical structure of PEG-*b*-PHEG and schematic representation of helix–coil transition for PHEG block.

EXPERIMENTAL

Materials

One-end aminated PEG (nominal molecular weight and its distribution index M_w/M_n are 5,500 and 1.08, respectively) was purchased from Shearwater, and used after fractional precipitation by dichloromethane (DCM)/petrorium ether. *N*-carboxyanhydride (NCA) of γ-benzyl L-glutamate (BLG) was prepared by reacting BLG with triphosgene,[34] and purified by recrystallization from tetrahydrofurane/petrorium ether. Cyclohexanol was dried with calcium hydride and distilled before use. Distilled water was ion-exchanged before use.

Synthesis of PEG-b-PHEG

NCA of BLG was polymerized with using the one-end aminated PEG in dry DCM at room temperature for four days. The solution was poured into diethyl ether, and precipitated polymers was re-precipitated by *N*,*N*-dimethyformamide (DMF)/water in order to remove unreacted PEG. Obtained poly(ethylene glycol)-*block*-poly(γ-benzyl L-glutamate) (PEG-*b*-PBLG) was dissolved in 2-aminoethanol/DMF (50:50 vol %) with polymer concentration of 0.1 g/mL, and side-chain exchanging reaction was performed for two days at room temperature.[35] The reacted solution was dialyzed against water by using cellulose membrane with nominal fractional molecular weight of 3,500. PEG-*b*-PHEG was obtained after freeze-drying of aqueous polymer solution.

Measurements

Viscosity and density of cyclohexanol/water mixed solvents were measured on Ubbelohde-type viscometer and density/specific gravity meter (DA-130, Kyoto Electronics Manufacturing), respectively. ^{1}H NMR spectrum of PEG-*b*-PHEG was recorded on JNM-GX400 (JEOL) with using DMSO-d_6 as solvent. SEC chart was recorded on SC-8020 (Toso). Eluent solvent was DMF/LiBr, and standard polystyrene was used for molecular weight calibration. Circular dichroism (CD) measurements were performed on J-820/805 (JASCO) with using a quartz cell having path length of 1 mm.

Light scattering was measured by a laboratory-made apparatus equipped with ALV/SO-SIPD detector and ALV-5000 correlator using He–Ne laser (wavelength $\lambda_0 = 633$ nm) as light source.[36,37] Sample solutions were optically purified by Millipore filter of nominal pore size of 0.45 or 1.0 μm and transferred into optical tube, and the tube was flame-sealed under gentle vacuum. Weight averaged molecular weight (M_w) and radius of gyration (R_g) were evaluated by excess Rayleigh ratio $R(\theta)$ calculated from measured excess scattering intensity as a function of scattering angle, θ. Extrapolation to dilute limit was not performed because of a possibility of concentration dependence of association behavior, therefore, evaluated results are apparent ones defined as

$$M_{w,app} = \frac{R(0)}{Kc} \quad (1)$$

$$R_{g,app}{}^2 = \frac{3\lambda_0{}^2 M_{w,app}(\text{initial slop})}{16\pi^2 n^2} \quad (2)$$

where the constant K is given by

$$K = \frac{4\pi^2 n^2 (dn/dc)^2}{N_A \lambda_0{}^4} \quad (3)$$

with n the refractive index of solvent, dn/dc the refractive index increment, and N_A the Avogadro constant. $Kc/R(0)$ and (initial slope) are intercept and initial slope of $Kc/R(\theta)$ *vs.* $\sin^2(\theta/2)$ plots at a finite concentration, c. Refractive indexes for PEG-*b*-PHEG and cyclohexanol/water were evaluated from those for PEG, PHEG, cyclohexanol and water[33,38] with assuming additional rule for the constitutional components. In dynamic light scattering measurements, correlation function of electric field was obtained from auto-correlation function of the scattered light intensity. Distribution of decay rate Γ was calculated by using CONTIN program, and transformed to hydrodynamic radius (R_h) with using Einstein–Stokes equation,

$$R_{h,app} = \frac{kT}{6\pi\eta D} = \frac{kT}{6\pi\eta(\Gamma/q^2)} \quad (4)$$

where $D = \Gamma/q^2$ the diffusion coefficient, η the solvent viscosity, k the Boltzmann constant, T the absolute temperature, and q the scattering vector given by

$$q = \frac{4\pi n \sin(\theta/2)}{\lambda_0}. \quad (5)$$

Because the measurements were performed at a finite concentration, evaluated hydrodynamic radius was also apparent one.

Concentration of polymer solution for CD and light scattering measurements was *ca.* 0.05 or 0.1 wt %, and temperature for these measurements was maintained at 30 °C.

Table I. Molecular weight and its distribution of PEG-*b*-PBLG and PEG-*b*-PHEG

Sample	M_n[a]			M_w/M_n[b]
	PEG	PBLG	PHEG	
PEG-*b*-PBLG	5,500	21,000		1.52
PEG-*b*-PHEG	5,500		7,500	1.56

[a] ^{1}H NMR. [b] SEC.

RESULTS

Characteristics of Polymers

^{1}H NMR spectrum for PEG-*b*-PHEG revealed complete exchange of benzyl side chains of PBLG to hydroxyethyl groups. Number averaged molecular weight M_n determined by ^{1}H NMR spectrum is listed in Table I. Decrease in M_n after the reaction from PEG-*b*-PBLG to PEG-*b*-PHEG suggests a possibility of main-chain scission during the side-chain exchanging reaction using 2-aminoethanol. However, after removal of lower molecular weight component by dialysis tube having cutoff molecular weight of 3,500, SEC diagram revealed single peak with $M_w/M_n = 1.56$.

Viscosity of Cyclohexanol/Water Mixture

It should be noted that cyclohexanol/water system occurs macrophase separation into cyclohexanol-rich and water-rich phases.[39] Cyclohexanol/water single phase can be obtained when the water content (w) is lower than 11.6 wt % at 30 °C. In order for analysis of dynamic light scattering results, viscosity measurement for the mixed solvent in one-phase region was conducted. Correction according to density difference was also conducted. Obtained relationship between w (wt %) and viscosity η (cP) at 30 °C can be expressed by the following equation.

$$\eta\ (\text{cP}) = 41.485 - 7.027w + 9.213 \times 10^{-1} w^2 - 7.289 \times 10^{-2} w^3 + 2.692 \times 10^{-3} w^4 \quad (6)$$

CD measurements and Helix–coil Transition

CD spectra for PEG-*b*-PHEG in cyclohexanol/water with polymer concentration of 0.05 wt % were measured with varying w from 2.3 to 12.1 wt %, and results are shown in Figure 2. When $w = 2.3$ and 4.1 wt %, two minima in the mean residual ellipticity ([Θ]) were observed at wavelength $\lambda = 208$ and 222 nm. With the increase of w, the minimum at 208 nm became broad and [Θ] value at 222 nm increased. It is reported that single-minimum spectrum is observed when CD-active chains are associated in solution.[40–43] Solution of $w = 12.1$ wt % exhibit typical CD spectrum for randomly coiled polypeptide.

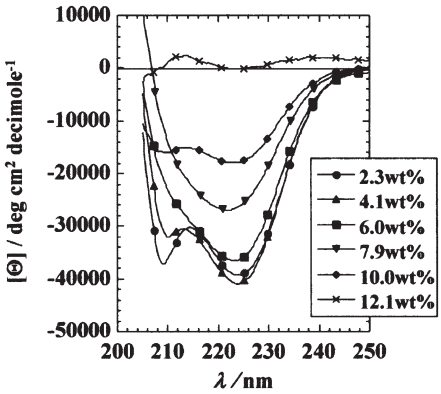

Figure 2. CD spectra for PEG-*b*-PHEG in cyclohexanol/water mixed solvent at 30 °C. Polymer concentrations are *ca.* 0.05 wt % for all solutions. Water contents in the mixed solvents, *w*, are (●) 2.3 wt %, (▲) 4.1 wt %, (■) 6.0 wt %, (▼) 7.9 wt %, (◆) 10.0 wt %, and (×) 12.1 wt %.

Table II. Numerical results of CD and light scattering measurements for PEG-*b*-PHEG micelles in cyclohexanol/water mixed solvents with different water content

w (wt %)	*c* (wt %)	f^H (%)	$M_{w,app}$ (10^6 g mol^{-1})	$R_{g,app}$ (nm)	$R_{h,app}$ (nm)
c = 0.05 wt %					
2.3	0.0509	96	274	129	79
4.1	0.0550	100	89.2	77	66
6.0	0.0540	91	24.3	54	54
7.9	0.0531	67	67.6	107	87
10.0	0.0450	45	2.4	98	58
12.1	0.0588	0	—	—	250
c = 0.1 wt %					
4.2	0.0995	99	944	140	112
12.2	0.104	1	—	—	363

The helix content f^H of PHEG was evaluated from [Θ] value at $\lambda = 222$ nm, $[\Theta]_{222}$ (deg cm^2 dmol^{-1}), as follows.[31]

$$f^H = \frac{[\Theta]_{222}}{-40{,}000} \tag{7}$$

Results are listed in Table II, and in Figure 3, f^H values are plotted against *w*. This figure clearly shows that PHEG chains are in α-helix state when $w = 2.3$ and 4.1 wt %, contains fairly amount of random-coil conformation when $w = 6.0$, 7.9, and 10.0 wt %, and completely in random-coil state when $w = 12.1$ wt %.

Static and Dynamic Light Scattering

Light scattering measurements for solutions with polymer concentration of *ca.* 0.05 wt % were performed with changing water content *w*, and evaluated $M_{w,app}$ and $R_{g,app}$ are listed in the upper part of Table II. As mentioned above, cyclohexanol/water mixture with $w = 12.1$ wt % is turbid and reveals

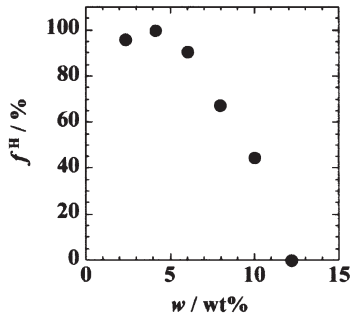

Figure 3. Plots of helix content f^H for PHEG block in PEG-*b*-PHEG dissolved in cyclohexanol/water mixed solvent against *w*.

phase separation into water-rich and cyclohexanol-rich macrophases. However, addition of small amount of PEG-*b*-PHEG makes the solution clear because of its ability as surfactant. It should be plausible that the water-rich phase is emulsified by PEG-*b*-PHEG, and PEG and PHEG blocks mainly exist in cyclohexanol-rich and water-rich phases, respectively. The $Kc/R(\theta)$ *vs.* $\sin^2(\theta/2)$ plot for this emulsified solution gave negative intercept, which may be owing to presence of large emulsions stabilized by PEG-*b*-PHEG localized at its interface. This assumption also explains the result of CD measurement, *i.e.*, PHEG chains take random-coil conformation because they locate in the water-rich phase.

All of the measured $R_{g,app}$ values are larger than 54 nm, which is larger than sum of chain length of the fully extended PEG (45.0 nm, calculated by using standard bond length and bond angle[44]) and α-helical PHEG (6.5 nm, calculated by using residual pitch for α-helix[45]). Therefore, a simple core-corona type spherical micelle is not plausible. In Figure 4, inverse of apparent particle scattering function defined by

$$P_{app}(q) = R(q)/R(0) \tag{8}$$

is plotted against $qR_{g,app}$, and compared with those of some structure models such as uniform sphere, infinitely-thin disc, and rigid rod with infinitely thin.[46] Figure 4 suggests that the observed scattering function showed good resemblance to that for infinitely-thin rigid rod model. Therefore, possible micelle structure formed in the solution with $w = 2.3$–10.0 wt % may be a cylindrical shape.

Distribution of decay rate Γ evaluated by dynamic light scattering measurements conducted at $\theta = 90°$ was converted to distribution of R_h, and typical examples are shown in Figure 5. For $w = 2.3$–10.0 wt % solutions, an unimodal distribution peak locates in the range of $R_{h,app} = 50$–90 nm, however, peak for $w = 12.1$ wt % solution locates around $R_{h,app} = 250$ nm. This result is also consistent with the static light scattering measurements as mentioned above, *i.e.*, relatively large water-rich phases are emulsified by

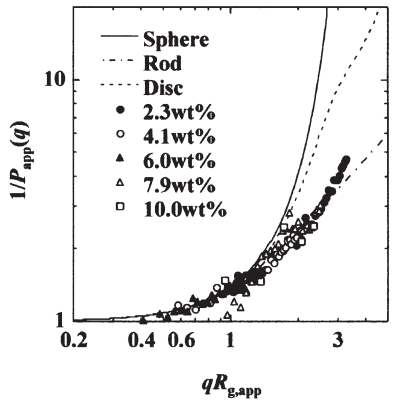

Figure 4. Plots of apparent scattering function $P_{app}(q)$ for PEG-*b*-PHEG micelles in cyclohexanol/water at 30 °C against $qR_{g,app}$ compared with those calculated by some simple structure models; uniform sphere (—), infinitely-thin disc (- - -), and infinitely-thin rigid rod (-·-·-). Polymer concentration is *ca.* 0.05 wt %. The plots are for solutions of $w = 2.3$ (●), 4.1 (○), 6.0 (▲), 7.9 (△), and 10.0 wt % (□).

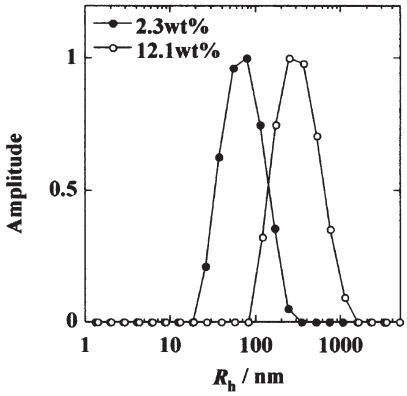

Figure 5. Distribution of hydrodynamic radius R_h by dynamic light scattering at $\theta = 90°$ for PEG-*b*-PHEG micelles in cyclohexanol/water with $w = 2.3$ wt % (●) and 12.1 wt % (○) measured at 30 °C. Polymer concentration is *ca.* 0.05 wt %.

PEG-*b*-PHEG. Because the angular dependence of $R_{h,app}$ was small, $R_{h,app}$ values obtained at $\theta = 90°$ are listed in Table II.

Concentration Dependence

In order to investigate concentration dependence of association behavior, solutions with 0.1 wt % polymer concentration have been prepared. However, completely clear solutions could not be prepared for mixed solvents with w close to 2, 6, 8 and 10 wt %, and some precipitates were remained. CD and light scattering measurements were performed for $w = 4.2$ and 12.2 wt % solutions, in which PEG-*b*-PHEG was completely dissolved, and numerical results are listed in the lower part in Table II. When w is *ca.* 4 wt %, f^H value kept almost 100%, and $M_{w,app}$, $R_{g,app}$ and $R_{h,app}$ values became larger with the increase of

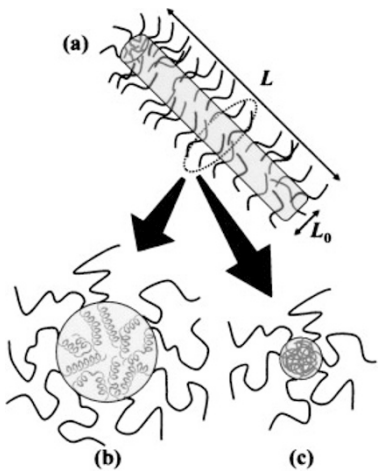

Figure 6. (a) Illustration of core-corona type cylindrical micelle with contour length L and diameter L_0 for core region. Estimated packing manner of PHEG in the core region are illustrated in cross-section, (b) when the helix content is in the range of $70\% \leq f^H \leq 90\%$ in solutions with $w = 6$ and 8 wt %, and (c) when $f^H = 45\%$ in solution with $w = 10$ wt %.

polymer concentration. Plot of scattering function $1/P_{app}(q)$ *vs.* $qR_{g,app}$ also suggested rigid-rod for micellar structure (data are not shown). Formation of large emulsions was also suggested for $w = 12.2$ wt % solution, *i.e.*, static light scattering analysis failed the extrapolation to zero angle and R_h distribution peak located at 363 nm.

DISCUSSION

As pointed out above, the observed $R_{g,app}$ values are larger than those assuming conventional core-corona type spherical micelle. The scattering function was closest to that for a thin-rod model as shown in Figure 4. In the following, the most plausible structure of cylindrical micelles will be estimated from the observed values of $R_{g,app}$ and $M_{w,app}$.

Schematic representation of core-corona type cylindrical micelle, with PHEG associated core and PEG corona, is illustrated in Figure 6a. Under an assumption of uniform density in a cylindrical core, contour length (L) and diameter (L_0) of the micelle core can be evaluated from the experimental $M_{w,app}$ by using next equation.

$$M_{w,core} = 0.58 M_{w,app} = N_A \rho \pi \left(\frac{L_0}{2}\right)^2 L \qquad (9)$$

where 0.58 is the weight fraction of PHEG in PEG-*b*-PHEG, and $\rho = 1.399\ g\,cm^{-3}$ is density of PHEG.[32] For rigid rodlike particle, relationship between $R_{g,core}$, L, and L_0 is expressed as follows.

$$R_{g,core}{}^2 = \frac{1}{2}\left(\frac{L_0}{2}\right)^2 + \frac{1}{12}L^2 \qquad (10)$$

Table III. Evaluated values of contour length (L) and diameter (L_0) of cylindrical micelles with assuming core-corona type structure

	Rigid-rod cylinder	
w (wt %)	L (nm)	L_0 (nm)
$c = 0.05$ wt %		
2.3	446	23.1
4.1	267	17.0
6.0	188	10.6
7.9	370	12.6
10.0	341	2.5
$c = 0.1$ wt %		
4.2	482	41.5

In calculation, $R_{g,core}$ was assumed to be equal to the observed value of $R_{g,app}$ because the contribution of PEG with $M_w = 5{,}500$ on $R_{g,core}$ should be small. Results for solutions with polymer concentration of 0.05 wt % are listed in the upper part of Table III. The diameter L_0 of the core can be compared with molecular geometry of PHEG. As mentioned above, molecular length along the α-helical PHEG is 6.5 nm. For randomly-coiled PHEG, R_g is calculated as 1.7 nm by using the characteristic ratio of end-to-end distance, $\langle r^2\rangle/nl^2 = 6.6$.[47] The L_0 values of 23.1 and 17.0 nm for $w = 2.3$ and 4.1 wt % solutions seems too large to be assuming uniformly packed PHEG core, so, the core-corona type cylindrical micellar model is not plausible for these solutions. For the solutions with $w = 6.0$ and 7.9 wt %, the evaluated L_0 is close to twice of the chain length of PHEG (13.0 nm). Because the helix content for these solutions is still high, core diameter may be determined by α-helical chain and packing manner of PHEG is possibly illustrated as shown in Figure 6b. Further increase of w to 10.0 wt % induced the decrease in $M_{w,app}$ with maintaining $R_{g,app}$ value, which suggests the decrease in core diameter. The L_0 value of 2.5 nm is comparable to R_g for random coil PHEG calculated above. Therefore, the decrease in f^H made it possible to form densely packed and slim core with randomly-coiled PHEG as shown in Figure 6c.

As shown in Table II, the value of $R_{g,app}/R_{h,app}$, which is used to elucidate the shape of the particle,[46] ranges from 1.0 to 1.7. These values are smaller than that expected for rigid rod (> 2.0), so there is possibility that the cylindrical micelles have some flexibility. For worm-like chain with persistence length P, the relation between $R_{g,core}$ and L can be expressed as follows.[4,48]

$$R_{g,core}{}^2 = P^2\left[\frac{L}{3P} - 1 + \frac{2P}{L} - \frac{2\{1 - \exp(-L/P)\}}{(L/P)^2}\right] \tag{11}$$

With assuming L_0 value, we can evaluate L and P from eqs 9 and 11. For $w = 2.3$ and 4.1 wt % solutions, L_0 was assumed to be twice of the chain length of α-helical PHEG (13.0 nm) because f^H are almost 100%. Thus obtained L values were more than ten times larger than P, *i.e.*, the micelle has much larger contour length than its persistence length. This result is inconsistent with the assumption that the micelle is rigid rod, thus, the core-corona type semiflexible cylindrical model is also implausible when $w = 2.3$ and 4.1 wt %. These calculations indicated that small decrease of L_0 resulted in drastic decrease of P. For $w = 6.0$ wt % solution, decrease in L_0 from 10.6 to 10.0 nm changed P value from ∞ to 164 nm, means that $M_{w,app}$ and $R_{g,app}$ for $w = 6.0$, 7.9, and 10.0 wt % solutions can be reasonably reproduced by semiflexible worm-like model. This flexibility of the cylindrical micelle may be having an effect on the value of $R_{g,app}/R_{h,app}$.

In order to reproduce the large $M_{w,app}$ values for solutions with small w, a rodlike vesicle model with a hollow cylinder having a pair of hollow hemispheres at its both ends has been examined. $M_{w,core}$ and $R_{g,core}$ for a rigid hollow hemispherical cylinder with inside radius r_1, outside radius r_0, and length of $L + 2r_0$ (see Figure 7) can be expressed as follows.

$$M_{w,core} = N_A\rho\left[\frac{4}{3}\pi\{{r_0}^3 - {r_1}^3\} + \pi L\{{r_0}^2 - {r_1}^2\}\right] \tag{12}$$

$$R_{g,core}{}^2 = \frac{\frac{4}{5}({r_0}^5 - {r_1}^5) + L({r_0}^4 - {r_1}^4) + \frac{L^2}{3}({r_0}^3 - {r_1}^3) + \frac{L^3}{12}({r_0}^2 - {r_1}^2)}{\frac{4}{3}({r_0}^3 - {r_1}^3) + L({r_0}^2 - {r_1}^2)} \tag{13}$$

By using the experimental $M_{w,app}$ and $R_{g,app}$ values, the geometrical parameters can be evaluated when the value of $r_0 - r_1$, which corresponds to the thickness of the PHEG associated domain of the hollow cylinder, is fixed. Under the assumption that $r_0 - r_1$ is equal to the chain length of α-helical PHEG (6.5 nm), diameter and length of the hollow cylinder can be obtained as listed in Table IV. The inner diam-

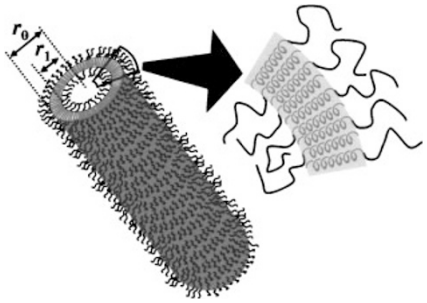

Figure 7. Illustration of hollow hemispherical cylinder micelle with inner radius r_1 and outer radius r_0 formed in solutions with $w = 2.3$ and 4.1 wt %. In PHEG associated domain, α-helical PHEG chains with $f^H = 100\%$ are arranged as their long axis aligned in monolayer manner.

Table IV. Evaluated values of inner radius (r_1), outer radius (r_0), and length along the cylinder (L) for the hollow cylindrical micelle with assuming the thickness for PHEG associated domain ($r_0 - r_1$) equal to 6.5 nm

w (wt %)	r_1 (nm)	r_0 (nm)	L (nm)
$c = 0.05$ wt %			
2.3	7.0	13.5	424
4.1	2.3	8.8	255
$c = 0.1$ wt %			
4.2	30.8	37.3	402

eters of the hollow cylinder are 14.0 and 4.6 nm for $w = 2.3$ and 4.1 wt % solutions, respectively, which is larger than R_g of the PEG (2.3 nm, evaluated by using $\langle r^2 \rangle / nl^2 = 4.0$). Thus, the vesicle-like structure model with monolayer packing as depicted in Figure 7 might be a possible structure for the rod–coil diblock copolymer micelles.

Table II shows that $M_{w,app}$ tends to decrease with the increase in w, although $R_{g,app}$ values revealed only small change. This result suggests the decrease in the diameter of the cylindrical micelles with the increase of w. As described in Introduction, packing manner of rod–coil diblock copolymers has been discussed theoretically and experimentally.[11–13,16–29] Rod blocks were proposed to be packing with their long axis aligned, and this packing manner induces a flat interface between rod- and coil-segregated domains. On the other hand, in random-coil polymer, it should be possible to form a segregated domain with large curvature such as spherical micelle. These considerations reveal good consistency with the micellar structures evaluated in this study. The vesicle-like micelle in which PHEG associated domains has smaller curvature is suggested when $f^H = 100\%$, and with the decrease of f^H, core-corona type cylindrical micelle in which PHEG domain has larger curvature was supposed to be formed. As pointed out in refs 32 and 33, cooperativity of helix–coil transition of PHEG is relatively weak, so it is suggested that α-helix sequences and random-coil sequences are coexisting in one PHEG chain. The small L_0 value for $w = 10.0$ wt % solution may suggest that PHEG chain cannot be regarded as rigid rodlike polymer and behaves as random coil when the helix content is smaller than 45%. Recently, Bellomo *et al.*[49] have reported that α-helical amphiphilic diblock copolypeptides form spherical vesicles with micrometer scale, however, such kind of vesicles could not be observed in samples prepared with using racemic amino acid. They pointed out the importance of helical conformation for the formation of flat membranes of giant vesicles. Although the length scale of the associates is different, their results showed similar tendency with our present work.

It should be noted that the above analysis of the scattering data assumes a simplified structure model for the micelles, *i.e.*, without size distribution. As shown in the R_h distribution in Figure 5, the micelle exists as polydisperse one. Thus, the comparison of scattering function in Figure 4 as well as the numerical results listed in Tables III and IV should be containing some uncertainty. The lack of the extrapolation to infinitely dilute limit also influence the evaluated results from the light scattering measurements. However, the tendency of the decrease in $M_{w,app}$ with the increase of w and decrease of f^H is suggested in Table II, and it can be described by the change of diameter of the cylindrical micelle and curvature for the PHEG associated domains as discussed above. We also performed similar elucidation for structural parameters with assuming spherical or disklike oblate shape for micelles, but the cylindrical model described above was most reasonable. This result is consistent with the comparison of experimental and theoretical $P_{app}(q)$ shown in Figure 4. Therefore, effect of the micellar size distribution on $qR_{g,app}$-dependence of $P(q)$ was not significant in this system.

Above considerations for micellar structure were also applied for 0.1 wt % solution with $w = 4.2$ wt %. As listed in Table III, the evaluated L_0 with assuming the core-corona type cylinder was larger than the chain length of α-helical PHEG. On the other hand, assumption of hollow cylinder gave a reasonable r_1 value (Table IV). Therefore, as like the more dilute solution, PEG-*b*-PHEG in 0.1 wt % solution most probably forms vesicle-like hollow cylindrical micelle when $w = 4.1$ wt %.

In the above discussion, structure change of the micelles is considered to be responsible to the conformational change of the core-forming PHEG block. Another possible reason for the micellar structure change is solvent quality, which would be less selective with the increase of water content. If PHEG be-

comes more soluble with the increase of w, the solvent molecules possibly enter into the PHEG domain. This swelling effect of PHEG core also makes it possible to form the PHEG domain with larger curvature. However, as mentioned above, it was difficult to prepare clear solutions with polymer concentration higher than 0.05 wt %. Because PEG is well dissolved in both water and cyclohexanol, this difficulty in solution preparation should be the result of poor solubility of PHEG block. Therefore, the swelling of PHEG domain may be playing minor role for the micellar structure change.

CONCLUSIONS

Structure of PEG-*b*-PHEG self-assembled micelles in dilute solution of cyclohexanol/water mixed solvent has been investigated. In this solvent system, PHEG block forms associated domains and PEG block is well dissolved. As shown by CD spectra in Figure 2, PHEG block changes its conformation from α-helix state to random coil state with the increasing of water content in the mixed solvent from 2.3 to 12.1 wt %. When $w = 2.3$ and 4.1 wt %, helix content f^{H} was almost 100% and micelle structure was supposed to be vesicle-like hollow hemispherical cylinder as illustrated in Figure 7. For solutions with $w = 6.0$, 7.9, and 10.0 wt %, f^{H} values decreased and PHEG blocks form densely-packed cylindrical core with smaller diameter, *i.e.*, the micelle is no longer hollow shape. These structure changes of micelles are interpreted by the conformational change of core-forming PHEG block. The parallel alignment of rigid-rod α-helix tends to make the PHEG domain more flat, and the small curvature for the core region results in vesicle-like hollow micelles. With the increase of flexibility, PHEG domains with larger curvature would be possibly formed. These results indicate that the conformation of the core-forming associated chains and their packing manner strongly influence the structure of diblock copolymer micelles.

Acknowledgment. This work was partly supported by Grant-in-Aid for Scientific Research from the Japan Society for the Promotion of Science (No. 15550105).

REFERENCES

1. I. W. Hamley, "The Physics of Block Copolymers," Oxford University Press, New York, N.Y., 1998.
2. Z. Tuzar and P. Kratochvil, in "Surface and Colloid Science," Vol. 15, E. Matijevic, Ed., Plenum Press, New York, N.Y., 1993, p 1.
3. K. Iyama and T. Nose, *Macromolecules*, **31**, 7356 (1998).
4. K. Iyama and T. Nose, *Polymer*, **39**, 651 (1998).
5. L. Zhang and A. Eisenberg, *Science*, **268**, 1728 (1995).
6. L. Zhang, K. Yu, and A. Eisenberg, *Science*, **272**, 1777 (1996).
7. L. Zhang and A. Eisenberg, *Macromolecules*, **32**, 2239 (1999).
8. M. Nakano, H. Matsuoka, H. Yamaoka, A. Poppe, and D. Richter, *Macromolecules*, **32**, 697 (1999).
9. M. Nakano, K. Matsumoto, H. Matsuoka, and H. Yamaoka, *Macromolecules*, **32**, 4023 (1999).
10. E. Minatti, P. Viville, R. Borsali, M. Schappacher, A. Deffieux, and R. Lazzaroni, *Macromolecules*, **36**, 4125 (2003).
11. M. Lee, B.-K. Cho, and W.-C. Zin, *Chem. Rev.*, **101**, 3869 (2001).
12. B. R. M. Gallot, *Adv. Polym. Sci.*, **29**, 85 (1978).
13. L. H. Radzilowski, J. L. Wu, and S. I. Stupp, *Macromolecules*, **26**, 879 (1993).
14. P. J. Flory, *Proc. R. Soc. London, Ser. A*, **234**, 73 (1956).
15. P. J. Flory, *Adv. Polym. Sci.*, **59**, 1 (1984).
16. A. N. Semenov and S. V. Vasilenko, *Sov. Phys. JETP*, **63**, 70 (1986).
17. A. Halperin, *Macromolecules*, **23**, 2724 (1990).
18. D. R. M. Williams and G. H. Fredrickson, *Macromolecules*, **25**, 3561 (1992).
19. P. Adriani, Y. Wang, and W. L. Mattice, *J. Chem. Phys.*, **100**, 7718 (1994).
20. A. Harada, S. Cammas, and K. Kataoka, *Macromolecules*, **29**, 6183 (1996).
21. K. Kataoka, A. Ishihara, A. Harada, and H. Miyazaki, *Macromolecules*, **31**, 6071 (1998).
22. S. A. Jenekhe and X. L. Chen, *Science*, **279**, 1903 (1998).
23. S. A. Jenekhe and X. L. Chen, *Science*, **283**, 372 (1999).
24. C. Wu, A. Niu, L. M. Leung, and T. S. Lam, *J. Am. Chem. Soc.*, **121**, 1954 (1999).
25. N. A. J. M. Sommerdijk, S. J. Holder, R. C. Hiorns, R. G. Jones, and R. J. M. Nolte, *Macromolecules*, **33**, 8289 (2000).
26. Y. Tu, X. Wan, D. Zhang, Q. Zhou, and C. Wu, *J. Am. Chem. Soc.*, **122**, 10201 (2000).
27. Y. Tu, X. Wan, H. Zhang, X. Fan, X. Chen, Q.-F. Zhou, and K. Chau, *Macromolecules*, **36**, 6565 (2003).
28. J. Wu, E. M. Pearce, T. K. Kwei, A. A. Lefebvre, and N. P. Balsara, *Macromolecules*, **35**, 1791 (2002).
29. F. Chécot, S. Lecommandoux, Y. Gnanou, and H.-A. Klok, *Angew. Chem., Int. Ed.*, **41**, 1340 (2002).
30. N. Lotan, A. Yaron, and A. Berger, *Biopolymers*, **4**, 365 (1966).
31. A. J. Adler, R. Hoving, J. Potter, M. Wells, and G. D. Fasman, *J. Am. Chem. Soc.*, **90**, 4736 (1968).
32. M. Miyake, S. Akita, A. Teramoto, T. Norisuye, and H. Fujita, *Biopolymers*, **13**, 1173 (1974).
33. T. Ohta, T. Norisuye, A. Teramoto, and H. Fujita, *Polym. J.*, **8**, 281 (1976).
34. W. H. Daly and D. Poche, *Tetrahedron Lett.*, **29**, 5859 (1988).
35. D. Nosková, R. Kotva, and F. Rypáček, *Polymer*, **29**, 2072 (1988).
36. R. Yamazaki, K. Inomata, and T. Nose, *Polymer*, **43**, 3647 (2002).

37. M. Itakura, K. Inomata, and T. Nose, *Polymer*, **42**, 9261 (2001).
38. S. Michielsen, in "Polymer Handbook," 4th ed., J. Brandrup, E. H. Immergut, and E. A. Grulke, Ed., Wiley-Interscience, New York, N.Y., 1999, p VII/547.
39. H. Stephen and T. Stephen, Ed., "Solubilities of Inorganic and Organic Compounds," Vol. 1, Pergamon, London, U.K., 1963.
40. W. L. Mattice, R. W. McCord, and P. M. Shippey, *Biopolymers*, **18**, 723 (1979).
41. O. Pieroni, A. Fissi, J. L. Houben, and F. Ciardelli, *J. Am. Chem. Soc.*, **107**, 2990 (1985).
42. D. Chung, S. Higuchi, M. Maeda, and S. Inoue, *J. Am. Chem. Soc.*, **108**, 5823 (1986).
43. H. Maeda, H. Kato, and S. Ikeda, *Biopolymers*, **23**, 1333 (1984).
44. P. J. Flory, "Statistical Mechanics of Chain Molecules," John Wiley & Sons, New York, N.Y., 1969.
45. P. Spadon, A. S. Verdini, and A. Del Pra, *Biopolymers*, **17**, 2029 (1978).
46. W. Burchard, *Adv. Polym. Sci.*, **48**, 1 (1983).
47. M. Oka, T. Hayashi, and A. Nakajima, *Polym. J.*, **17**, 621 (1985).
48. S. A. Allison, S. S. Sorlie, and R. Pecora, *Macromolecules*, **23**, 1110 (1990).
49. E. G. Bellomo, M. D. Wyrsta, L. Pakstis, D. J. Pochan, and T. J. Deming, *Nat. Mater.*, **3**, 244 (2004).